Structure of Autocatalytically Branched Actin Solutions

A. E. Carlsson

Department of Physics, Washington University, St. Louis, Missouri 63130, USA

(Received 20 January 2004; published 10 June 2004)

The average branching number and cluster size in branched actin solutions with filament capping are evaluated using analytic theory and simulation methods. The average number of daughter branches per filament in steady state is much less than unity, regardless of the concentration of branching stimulant. Much more highly branched structures are obtained in the initial stages of polymerization.

DOI: 10.1103/PhysRevLett.92.238102 PACS numbers: 87.16.–b, 82.35.–x, 87.15.–v

Motion and shape changes of crawling cells rely crucially on force generation by polymerization of the protein actin into semiflexible filaments [1]. The polymerization is often induced by filament branching, which occurs autocatalytically in the sense that the generation rate for new filaments is enhanced by preexisting filaments. Complex supramolecular actin structures, such as highly branched networks, are formed by the interplay of molecular-scale processes including growth, branching, and filament capping. Our understanding of these intracellular processes is aided by the study of simple aqueous solutions including only actin and a few other proteins. The structure of such actin solutions is well understood for the case when only growth and capping are present. Branching has been included in recent continuum models of protein distributions in cells [2]. There have also been several experimental studies of the supramolecular structures induced by external bundling agents (see, for example, Refs. [3–5]). However, there has been no quantitative theoretical analysis of the interplay between branching, growth, and capping in determining the supramolecular structure of actin aggregates. This Letter presents such an analysis, using analytic theory and simulation methods to treat an actin polymerization model including the key types of topological and growth events.

The molecular-level events involved in actin-based motility have been treated in recent reviews [6–8]. Actin filaments are polar, with the two ends denoted "barbed" and "pointed"; barbed-end growth is more rapid, typically by a factor of about 10. Growth and depolymerization can be inhibited by the attachment of capping proteins or complexes, such as gelsolin and capping protein (CP) at the barbed end, and the Arp2/3 complex at the pointed end. The Arp2/3 complex also induces branch formation [9], probably along filament sides [10–13] (see, however, Ref. [14]). The Arp2/3 complex attaches to the side of a "mother" filament and binds the pointed end of a "daughter" filament. The Arp2/3 complex by itself is inactive, but extracellular stimuli can activate it inside the cell, and thus initiate branching and polymerization. The branches eventually dissociate from their mother filaments; this process can be accelerated by the presence of proteins such as ADF/cofilin [15].

I include these effects in a model of actin in solution with activated Arp2/3 complex and capping protein, similar to that used in recent studies of actin-based force generation [16–18]. The main processes in the model, filament growth, capping, and branching, are illustrated in Fig. 1. Filament growth occurs by diffusion of free actin monomers to filament ends, and is described by a net barbed-end monomer addition rate $k_{\mathrm{on}}^{\mathrm{B}} = k_0^{\mathrm{B}}([\mathrm{G}] - \mathrm{G}_{\mathrm{c}}^{\mathrm{B}})$ and a pointed-end depolymerization rate $k_{\mathrm{off}}^{\mathrm{P}} = k_0^{\mathrm{P}}(\mathrm{G}_{\mathrm{c}}^{\mathrm{P}} - [\mathrm{G}])$, where k_0^{B} and k_0^{P} are concentration-independent rate parameters, $[\mathrm{G}]$ is the free actin-monomer concentration, and $\mathrm{G}_{\mathrm{c}}^{\mathrm{B}}$ and $\mathrm{G}_{\mathrm{c}}^{\mathrm{P}}$ are the barbed- and pointed-end critical concentrations, which satisfy $\mathrm{G}_{\mathrm{c}}^{\mathrm{P}} > \mathrm{G}_{\mathrm{c}}^{\mathrm{B}}$. In steady state, $\mathrm{G}_{\mathrm{c}}^{\mathrm{B}} < [\mathrm{G}] < \mathrm{G}_{\mathrm{c}}^{\mathrm{P}}$. Capping is described by barbed- and pointed-end capping and uncapping rates $k_{\mathrm{cap}}^{\mathrm{B}} = k_{\mathrm{cap},0}^{\mathrm{B}}[\mathrm{CP}]$, $k_{\mathrm{uncap}}^{\mathrm{B}}$, $k_{\mathrm{cap}}^{\mathrm{P}} = k_{\mathrm{cap},0}^{\mathrm{P}}[\mathrm{Arp2/3}]$, and $k_{\mathrm{uncap}}^{\mathrm{P}}$, where $[\mathrm{CP}]$ is the concentration of capping protein, and $[\mathrm{Arp2/3}]$ is the concentration of the Arp2/3 complex. Branching is described by a branching rate per subunit in a filament, which has the form $k_{\mathrm{br}} = k_{\mathrm{br},0}[\mathrm{Arp2/3}]([\mathrm{G}] - \mathrm{G}_{\mathrm{c}}^{\mathrm{B}})^2$ for $[\mathrm{G}] > \mathrm{G}_{\mathrm{c}}^{\mathrm{B}}$ and $k_{\mathrm{br}} = 0$ for $[\mathrm{G}] < \mathrm{G}_{\mathrm{c}}^{\mathrm{B}}$. The power of 2 is

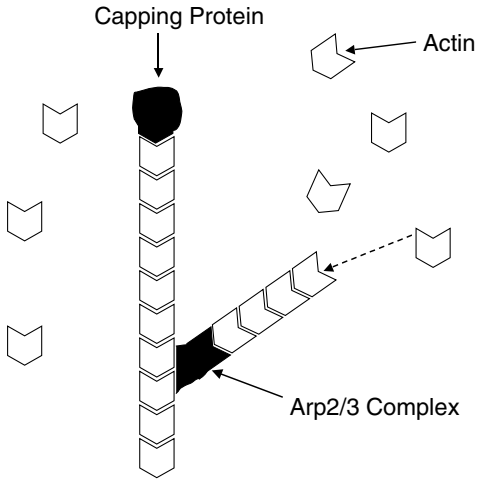

FIG. 1. Schematic of autocatalytic growth model.

taken from a recent kinetic analysis [13]. Debranching is described by a branch dissocation rate constant $\tau_{\rm dis}^{-1}$, which is independent of the actin concentrations. I ignore spontaneous nucleation of filaments, because branching nucleation is much faster.

The main property of interest here is the average number of branches growing from the side of a typical filament, which I denote $n_{\rm br}$. Intuitively, $n_{\rm br}$ should increase with increasing [Arp2/3]. I evaluate the steady-state value of $n_{\rm br}$ using a simple balance of filament creation and destruction, assuming the following filament "life cycle": A daughter filament is created by branching from a mother filament, with the Arp2/3 complex capping its pointed end. Next, its barbed end becomes capped. Subsequently, the filament dissociates from the mother filament and loses its pointed-end cap. Finally, it depolymerizes from the pointed end. I write the time rate of change of the total number of filaments N as a sum of creation and destruction terms:

$$dN/dt = k_{\rm br}\bar{l}N - N/(\tau_{\rm dis} + \tau_{\rm depol}), \tag{1}$$

where $\bar{l}$ is the average filament length (measured in subunits),

$$\tau_{\rm depol} = \bar{l}/(\eta_{\rm p}k_{\rm off}^{\rm P} - \eta_{\rm b}k_{\rm on}^{\rm B}) \tag{2}$$

is the average filament depolymerization time, and $\eta_{\rm b}$ and $\eta_{\rm p}$ are the probabilities that a filament's barbed and pointed ends, respectively, are uncapped. The first term on the right-hand side of Eq. (1) simply follows from the definition of $k_{\rm br}$. The second term states that the destruction of a filament requires both dissocation and depolymerization, sequentially. The time before the filament is capped is assumed to be a negligible part of the filament lifetime. According to the capping rates measured in Ref. [13] and the debranching rates measured in Ref. [19], this would hold for capping protein concentrations greater than 1 nM. The solution of a set of deterministic rate equations for the length distributions of four types of filaments (uncapped, pointed-end capped, barbed-end capped, and both-ends capped) shows that

$$\bar{l} = k_{\rm on}^{\rm B}/k_{\rm cap}^{\rm B} + \eta_{\rm b}k_{\rm on}^{\rm B}/(\eta_{\rm p}k_{\rm off}^{\rm P} - \eta_{\rm b}k_{\rm on}^{\rm B}). \tag{3}$$

The steady-state condition ($dN/dt = 0$) is then

$$k_{\rm br}\bar{l} = 1/(\tau_{\rm dis} + \tau_{\rm depol}). \tag{4}$$

Because of the dependences of the rate parameters on [G], this equation implicitly determines the critical concentration. To use it to calculate the number of branches $n_{\rm br}$ per filament, I balance filament creation and dissociation rates for branching on a single filament:

$$dn_{\rm br}/dt = k_{\rm br}\bar{l} - n_{\rm br}/\tau_{\rm dis}, \tag{5}$$

so that in steady state,

$$n_{\rm br} = \tau_{\rm dis}k_{\rm br}\bar{l}. \tag{6}$$

Combining Eqs. (4) and (6), I obtain

$$n_{\rm br} = \tau_{\rm dis}/(\tau_{\rm dis} + \tau_{\rm depol}) < 1, \tag{7}$$

so that $n_{\rm br}$ is simply the fraction of the total filament destruction time comprised by the dissociation time. Thus, in steady state, filaments must have less than one daughter filament on average. For reasonable values of the protein concentrations, $n_{\rm br} \ll 1$. For example, analysis of Eq. (1) using the parameters of Ref. [13] (ignoring barbed-end uncapping effects for simplicity) indicates that for $\tau_{\rm dis} \leq 1000$ s, $G_c - G_c^B \simeq (G_c^P - G_c^B)/(1 + 0.1x)$, where $x = [{\rm Arp2/3}]/[{\rm CP}]$. Combining this result with Eqs. (3) and (6) and the functional forms given for the branching, capping, and growth rates yields

$$n_{\rm br} = \frac{\tau_{\rm dis}k_{\rm br,0}k_0^{\rm B}(G_c^{\rm P} - G_c^{\rm B})^3 x}{k_{\rm cap,0}^{\rm B}(1 + 0.1x)^3}. \tag{8}$$

The maximum value of $x/(1 + 0.1x)^3$ is about 1.5, and using the parameters of Ref. [13] gives $n_{\rm br} \leq 0.12$. Because this result is based on the rate constants rather than the protein concentrations, it has quite general validity. I have found that plausible variations in the form of the branching rate cause only $\sim$20% changes in $n_{\rm br}$. Inclusion of additional proteins could increase $n_{\rm br}$. For example, addition of cortactin [19] should stabilize branches, and thus increase $\tau_{\rm dis}$ and $n_{\rm br}$.

These conclusions are supported by a more complete analysis based on stochastic simulation. The simulations use a methodology similar to that of Ref. [16], in which the coordinates of all filament subunits are stored over time. Filaments nucleate in random directions at random points in space, and subsequent branching, branch dissociation, growth, depolymerization, capping, and uncapping events are treated stochastically. I ignore interactions between subunits on distinct filaments because of the low volume fraction at typical *in vitro*

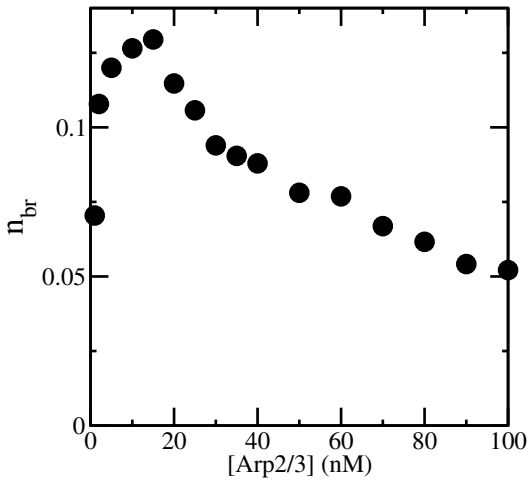

FIG. 2. Dependence of average number of daughter filaments per filament on [Arp2/3], for [CP] = 5 nM.

concentrations. Polymerization events remove free monomers from solution, and vice versa; [Arp2/3] and [CP] also vary with branching and capping events. The simulations treat actin concentrations up to 2 μM, in cubic regions of edge length 6 μm, containing up to about 250 000 actin monomers. The rate parameters are obtained from the kinetic fits of Ref. [13]. Figure 2 shows the dependence of n_{br} on [Arp2/3] for [CP] = 5 nM. n_{br} initially rises, then reaches a maximum of only 0.13 at [Arp2/3] $\simeq$ 20 nM, close to the above analytic estimate. It than slowly drops with increasing [Arp2/3].

These results raise two questions. First, why does increasing [Arp2/3] eventually lead to decreasing n_{br}? The main reason is that the barbed ends generated by new branches consume free monomers, reducing [G], and thereby reducing k_{br}. Equation (8) shows that the decreased value of [G] eventually outweighs the direct effect of increasing [Arp2/3]. The large sensitivity to [G] comes from the product $k_{\mathrm{br}}k_{\mathrm{on}}^{\mathrm{B}}$. The dependence of $k_{\mathrm{on}}^{\mathrm{B}}$ on [G] is well established. The [G] dependence of k_{br} is less certain, but any positive dependence of k_{br} on [G] would lead to an eventual decrease of n_{br} in Eq. (8).

The second question raised by the results is how highly branched actin networks ($n_{\mathrm{br}} \gg 1$) can form in cells and in related model systems, such as solutions containing protein-coated plastic beads. The answer is that the highly branched structures are dynamic in origin—they cannot persist in steady state. To demonstrate this, I have analyzed the structures induced by suddenly turning on branching, which could be taken to mimic the response of a cell to an external branching stimulus. Before branching is turned on, [G] is close to G_c^P because most of the barbed ends are capped, and the Arp2/3 complex is inactive. Shortly after branching begins, clusters of filaments form before debranching occurs and establishes steady state. I evaluate the average size N_{fil} (measured in filaments) to which a filament cluster grows before its first branch dissociation event, by initially ignoring the dissociation term in Eq. (1). Then $dN_{\mathrm{fil}}(t)/dt = \kappa N_{\mathrm{fil}}$, where $\kappa = k_{\mathrm{br}}\bar{l}$, and the parameters are evaluated using the initial value of [G] rather than the steady-state value. Cluster growth begins when the mother filament forms its first daughter filament, so that $N_{\mathrm{fil}}(0) = 2$. Then $N_{\mathrm{fil}}(t) = 2\exp(\kappa t)$. A reasonable criterion for the average time t_{dis} of the first debranching event is that the sum S of the ages of all the daughter filaments in the cluster should equal τ_{dis}. Since $dS/dt = N_{\mathrm{fil}} - 1$, the criterion becomes

$$\frac{2[\exp(\kappa t_{\mathrm{dis}}) - 1]}{\kappa} - t_{\mathrm{dis}} = \tau_{\mathrm{dis}}. \tag{9}$$

If $\tau_{\mathrm{dis}}\kappa \gg 1$ before the initiation of branching, which holds if [G] is large enough, the cluster size at the first debranching event is

$$N_{\mathrm{fil}}(t_{\mathrm{dis}}) \simeq \kappa\tau_{\mathrm{dis}}. \tag{10}$$

This yields $N_{\mathrm{fil}}(t_{\mathrm{dis}})$ values of about 20 for [CP] = 5 nM and 10 for [CP] = 10 nM, using [G] = 2 μM and [Arp2/3] = 14.3 nM. By comparison, evaluation of Eq. (9) at the steady-state critical concentrations gives $N_{\mathrm{fil}}(t_{\mathrm{dis}}) = 2.3$ and 2.2, respectively. Thus the early-time structure is much more highly branched than the steady-state structure.

To confirm this simplified analysis, I have simulated such a branching explosion using the stochastic growth methodology. Figure 3 shows the structure of the actin clusters for 2 μM actin, 5 nM CP, and 14.3 nM Arp2/3 complex, early in polymerization [3(a)] and after steady-state is reached [3(b)]. The large reduction of branching is apparent. In Fig. 4(a), I plot the time dependence of $\langle N_{\mathrm{fil}}^2\rangle^{1/2}$, where the average is over clusters. I use the root-mean-square form because this corresponds more closely to measurable quantities than would a linear average. As the above theory predicts, the average cluster

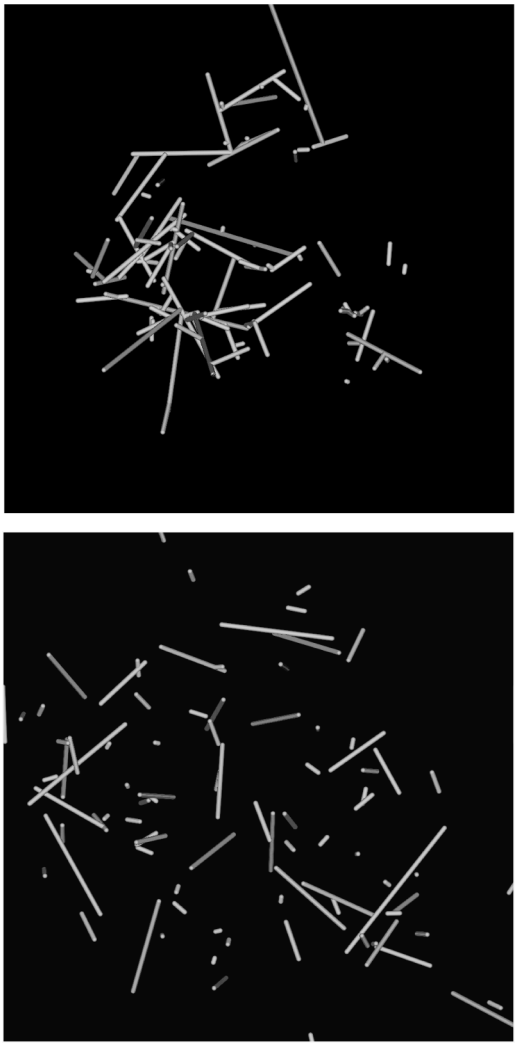

FIG. 3. Actin filament structure in early stage of polymerization (top) and in steady state (bottom), for [G] = 2 μM, [CP] = 5 nM, and [Arp2/3] = 14.3 nM.

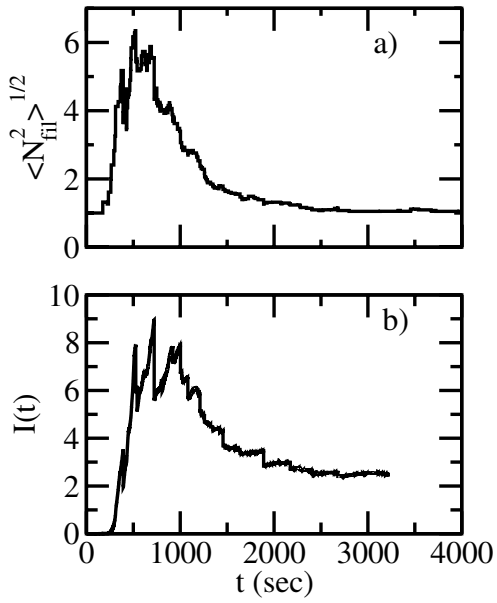

FIG. 4. Time dependence of root-mean-square number of filaments per cluster (a) and small-angle light-scattering intensity [(b), arbitrary units] vs time, for [G] = 2 μM, [CP] = 5 nM, and [Arp2/3] = 14.3 nM.

size grows to a peak in the initial stages of polymerization, and then drops down to the steady-state value near unity. These effects could be measured using small-angle light-scattering (SALS) methods. The average radius a of the clusters obtained here is typically less than 2 μm, for [CP] values of 5 μM or more. If $qa \ll 1$, where q is the scattering wave vector, and position correlations between clusters can be ignored, the scattered intensity I satisfies $I \propto \sum_i N_{\text{subunit}}(i)^2$, where $N_{\text{subunit}}(i)$ is the number of subunits in cluster i. Figure 4(b) shows that the branching explosion causes a marked peak in $I(t)$, so SALS experiments should give an unambiguous test of these effects.

The cytoplasm of a living cell contains higher concentrations of all the proteins considered here, and additional proteins, including ADF/cofilin and cortactin. It is also suspected that the rate of filament subunit branching decays over time [10,11]. Finally, the cytoplasm is very crowded because of the high volume fraction occupied by proteins. These effects do not change the conclusion that $n_{\text{br}} < 1$ [Eq. (7)], which is independent of the reaction rates and depends only on the general form of the model. The estimates given by Eq. (8) are, however, affected by the reaction rates. For example, τ_{dis} is reduced by ADF/cofilin and enhanced by cortactin. τ_{dis} in cells is probably much smaller than the *in vitro* value [15,19] of about 600 s used here, which would reduce n_{br}. The decay in the subunit branching rate over time would decrease $k_{\text{br},0}$, which according to Eq. (8) would also decrease n_{br}. Crowding by macromolecules should enhance the growth, capping, and branching rates because of excluded-volume effects. Actin polymerization data [20] suggest an increase of about a factor of 10 in the growth and capping rate constants of Eq. (8) at cellular concentrations. This factor cancels out of the ratio $k_0^{\text{B}}/k_{\text{cap},0}^{\text{B}}$. The reduced τ_{dis} in the cytoplasm could conceivably be countered by a very large increase of $k_{\text{br},0}$ due to crowding, but there is no evidence for such an increase. Thus, in steady state in the cell interior, actin filaments must have few branches and are likely mainly unbranched. The formation of highly branched structures in lamellipodia might then be interpreted as follows: The cell membrane is believed to activate filament branching. If newly formed filaments grow and push the network away from the membrane, the branching stimulus is dynamic in the sense that a given portion of the network branches only for a short period of time before it moves away from the membrane. This could allow the formation of highly branched structures.

I appreciate conversations with John Cooper and David Sept, and support from the National Science Foundation under Grant No. DMS-0240770.

[1] D. Bray, *Cell Movements: from Molecules to Motility* (Garland Publishing, New York, 2001).
[2] A. Mogilner and L. Edelstein-Keshet, Biophys. J. **83**, 1237 (2002).
[3] J. X. Tang and P. A. Janmey, J. Biol. Chem. **271**, 8556 (1996).
[4] A. Suzuki and T. Ito, Biochemistry (U.S.) **35**, 5245 (1996).
[5] G. C. L. Wong, A. Lin, J. X. Tang, Y. Li, P. A. Janmey, and C. R. Safinya, Phys. Rev. Lett. **91**, 018103 (2003).
[6] J. A. Cooper and D. A. Schafer, Curr. Opin. Cell Biol. **12**, 97 (2000).
[7] T. D. Pollard and G. G. Borisy, Cell **112**, 453 (2003).
[8] M.-F. Carlier, C. Le Clainche, S. Wiesner, and D. Pantaloni, BioEssays **25**, 336 (2003).
[9] R. D. Mullins, J. A. Heuser, and T. D. Pollard, Proc. Natl. Acad. Sci. U.S.A. **95**, 6181 (1998).
[10] K. J. Amann and T. D. Pollard, Proc. Natl. Acad. Sci. U.S.A. **98**, 15 009 (2001).
[11] I. Ichetovkin, W. Grant, and J. Condeelis, Curr. Biol. **12**, 79 (2002).
[12] I. Fujiwara, S. Suetsugu, S. Uemura, T. Takenawa, and S. Ishiwata, Biochem. Biophys. Res. Commun. **293**, 1550 (2002).
[13] A. E. Carlsson, M. A. Wear, and J. A. Cooper, Biophys. J. **86**, 1074 (2004).
[14] D. Pantaloni, R. Boujemaa, D. Didry, P. Gounon, and M.-F. Carlier, Nature Cell Biol. **2**, 385 (2000).
[15] L. Blanchoin, T. D. Pollard, and R. D. Mullins, Curr. Biol. **10**, 1273 (2000).
[16] A. E. Carlsson, Biophys. J. **81**, 1907 (2001).
[17] A. Mogilner and G. Oster, Biophys. J. **84**, 1591 (2003).
[18] A. E. Carlsson, Biophys. J. **84**, 2907 (2003).
[19] A. M. Weaver, A. V. Karginov, A. W. Kinley, S. A. Weed, Y. Li, J. T. Parsons, and J. A. Cooper, Curr. Biol. **11**, 370 (2001).
[20] D. Drenckhahn and T. D. Pollard, J. Biol. Chem. **261**, 12 754 (1986).